

## Evaluation of Operational Objective Streamline Methods

GARY L. ACHEMEIER

*Illinois State Water Survey, Urbana 61801*

(Manuscript received 8 May 1978; in final form 29 September 1978)

### ABSTRACT

Objective streamline analysis techniques are separated into predictor-only and predictor-corrector methods, and generalized error formulas are derived for each method. Theoretical analysis errors are obtained from the ellipse, hyperbola and sine wave curve families, curves which taken alone or in combination often describe many meteorological flow patterns. The predictor-only method always underestimated streamline curvature. The predictor-corrector method overestimated curvature where the step increment was directed toward increasing curvature and underestimated curvature where the step increment was directed toward decreasing curvature. This led to at least a partial compensation which reduced the cumulative error.

### 1. Introduction

The meteorological community's increased interest in weather systems that are characterized by large wind field divergences has led to the need for fast objective methods that give streamlines of the instantaneous flow. Streamlines have been essential to the understanding of mesoscale and cloud-scale flow patterns associated with severe thunderstorms (Barnes, 1974; Heymsfield, 1976). The relationship between surface convergence and convective rainfall over Florida has renewed interest in the surface wind field as a potential source of covariates in the evaluation of convective rainfall precipitation management experiments (Achtemeier *et al.*, 1978). The statistical design may also include real-time operational prestratification of days during which convective rainfall is expected.

Accurate, legible, real-time analyses of wind fields are essential to these evaluational and operational forecasts. Wind field streamlines at surface and above ground levels can reveal circulation centers, confluence and diffluence zones, and other wind field perturbations that might identify potential precipitation-producing weather systems. An automated streamline analysis releases valuable time of skilled meteorologists that would have been consumed in manually produced streamlines (Saucier, 1955). Further, the objective method should accurately describe the instantaneous wind field so as not to lead the forecast personnel to errors in pattern interpretations.

Objective streamline analyses schemes described in the literature fall into one of two categories: the predictor-only (PO) method in which line segments are extrapolated forward along the tangent to the

unit wind vector at the beginning point, and the predictor-corrector (PC) method which averages the wind direction angles at the beginning and ending points of the PO line segment and extrapolates line segments from the beginning point forward at the average angle. Predictor-only methods have been described by Davis (1969), Daart (1972) and Whitaker (1977). The NCAR scheme<sup>1</sup> and the method designated SLX in this paper are predictor-corrector methods.

This paper presents a theoretical error analysis that contrasts the PO and PC methods for analytical curves selected from the ellipse, hyperbola and sine wave curve families. These curves, occurring alone or in combination, often describe many meteorological flow patterns.

A general description of the SLX objective streamline analysis and an example analysis are presented in the Appendix.

### 2. Theoretical error analysis for the PO and PC methods

An automated streamline analysis technique should accurately describe the instantaneous flow field. Since the sequence of extrapolated line segments is an approximation to the true streamline, some analysis error should be expected. A foreknowledge of the magnitude and character of this error is essential in knowing the level of confidence that should be placed on an analysis. The analysis errors for known streamline equations have been obtained for the PO and PC methods. The character

<sup>1</sup> R. L. Lackman, personal communication on NCAR streamline program description.

of these errors gives some insight into the methods' limitations and reveals those areas of streamline fields which should be interpreted with caution.

Consider the subgrid square illustrated in Fig. 1. The corner angles  $\gamma_i, i = 1-4$ , have been found by bilinear interpolation from  $u$  and  $v$  components of the wind at points on the larger master grid. A schematic streamline enters the subgrid square at point A at an angle  $\alpha_b$ , determined from linear interpolation between the corner angles  $\gamma_i$  on the side of entry. A line segment tangent to the entry angle is extrapolated forward. This line intersects the opposite side of the subgrid square at C to form the PO method streamline segment. At C, the end-of-segment angle  $\alpha_e$  is found by linear interpolation between the corner angles on the side of exit. The segment begin and end angles are averaged and the PC segment is extrapolated forward at this angle  $\alpha_a$ . Perhaps the actual streamline entered the box at A and exited through B. Then the distance BC (BD) would be a measure of the PO (PC) method error for that subgrid box.

For an arbitrary predictor-corrector method, we approximate the chord angle  $\alpha_s$  by some linear combination of the begin-of-segment angle  $\alpha_b$  and the end-of-segment angle  $\alpha_e$ . Then the angular error between the approximated and true values of  $\alpha_s$  is given by

$$R = \alpha_s - (\alpha_b + W\alpha_e)/(1 + W). \tag{1}$$

$$R^* = \frac{2 \tan\alpha_s(1 - \tan\alpha_b \tan\alpha_e) - (1 - \tan^2\alpha_s)(\tan\alpha_b + \tan\alpha_e)}{(1 - \tan^2\alpha_s)(1 - \tan\alpha_b \tan\alpha_e) + 2 \tan\alpha_s(\tan\alpha_b + \tan\alpha_e)}. \tag{3}$$

To find the error for the predictor-only method ( $W = 0$ ), define  $R^+ = \tan R$  so that (1) becomes

$$R^+ = \tan(\alpha_s - \alpha_b). \tag{4}$$

Application of trigonometric identities gives the angular error

$$R^+ = \frac{\tan\alpha_s - \tan\alpha_b}{1 + \tan\alpha_s \tan\alpha_b} \tag{5}$$

for the PO method.

If the streamline that passes through points A and B in Fig. 1 is given by  $y = f(x)$  and the stream-

and (3) becomes

$$R^* = \frac{2\tilde{f}'(x)[1 - f'(x_1)g'(x_2)] - [1 - \tilde{f}'(x)^2][f'(x_1) + g'(x_2)]}{[1 - \tilde{f}'(x)^2][1 - f'(x_1)g'(x_2)] + 2\tilde{f}'(x)[f'(x_1) + g'(x_2)]}. \tag{8}$$

Given the appropriate analytical curves, Eqs. (7) and (8) can be solved for  $R^*$  and  $R^+$ . Then (1) will give the angular errors for each PO and PC streamline segment. For small angle errors, the streamline position error  $Z$  can be approximated by

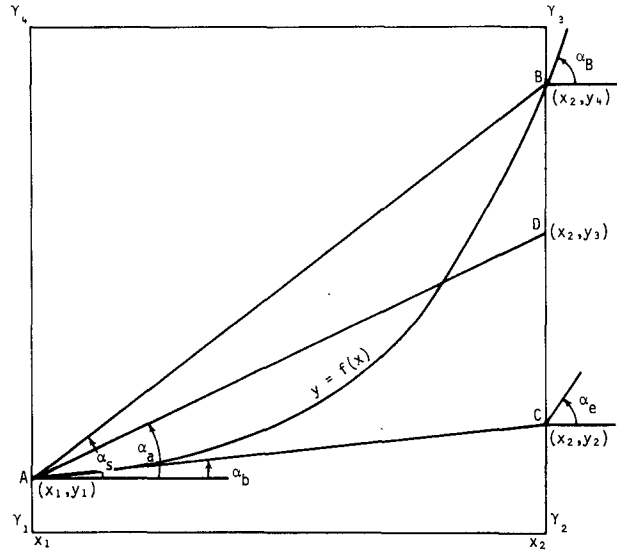


FIG. 1. Schematic diagram showing the method of approximation of a streamline in a subgrid square by straight line segments.

We then let  $R^* = \tan(2R)$ , so that

$$R^* = \tan[2\alpha_s - 2(\alpha_b + W\alpha_e)/(1 + W)]. \tag{2}$$

These angle sums and differences can be removed by the successive application of trigonometric identities. For the SLX predictor-corrector method,  $W = 1$ . Then  $R^*$  is expressed by

line that passes through point C is given by  $y = g(x)$ , the following are true:

$$\left. \begin{aligned} \alpha_b &= \arctan f'(x_1) \\ \alpha_e &= \arctan g'(x_2) \\ \alpha_s &= \arctan \left[ \frac{f(x_2) - f(x_1)}{x_2 - x_1} \right] = \arctan \tilde{f}'(x) \end{aligned} \right\} \tag{6}$$

It follows that (5) reduces to

$$R^+ = \frac{\tilde{f}'(x) - f'(x_1)}{1 + \tilde{f}'(x)f'(x_1)}, \tag{7}$$

$$Z = R \Delta x, \tag{9}$$

where  $\Delta x$  is the projection of the step increment length onto the  $x$  axis.

The total error between the analytical and extrap-

olated curves is given by the sum of the individual errors as the streamline passes through a succession of subgrid boxes. It is difficult to compute the total error from box to box because the streamline may enter or exit from the bottom or the top of the grid box. The  $\Delta x$  would have to be determined for both the true and extrapolated streamline for each box. Instead, (7) and (8) have been solved by stepping forward along the analytical curve in increments equal to one subgrid unit (1 SGU). This appears to be a reasonable assumption because the longest possible streamline segment is  $\sqrt{2}$  SGU along the subgrid box diagonal and many segments can be much shorter than 1 SGU.

The assumption that  $g(x) = f(x)$  further simplifies the computations. The additional error caused by making this assumption will be the subject of actual streamline calculations presented later in the next section.

### 3. Examples of the error analysis for selected curves

Predictor-only and predictor-corrector errors were computed for analytical curves selected from the ellipse, hyperbola and sine wave curve families. These curves often resemble atmospheric flow patterns. The various amplitudes and curvatures were chosen so that the curves would be representative of wind field patterns as analyzed onto the master grid and that the scale of the curves would be small enough to reveal the weaknesses of the two methods. We assume that the smallest resolvable wavelength is two master grid spaces. The subgrid resolution of this wave is dependent on the choice of the length of the subgrid unit.

$$R^* = \frac{\epsilon(1 - \epsilon^2)(x_2 - x_1)[2a^2(\beta_1 - \beta_2) + (x_2 + x_1)(x_1\beta_2 - x_2\beta_1)]}{(1 - \epsilon^2)[(x_2 - x_1)^2(-\epsilon^2\beta_1\beta_2 - x_1x_2) + 2x_1x_2(x_1x_2 - \beta_1\beta_2 + a^2)] + 2\epsilon^2a^2(-\beta_1\beta_2 + a^2 - x_1x_2)} \quad (14)$$

When  $\epsilon = 0$ , the ellipse reduces to a straight line. Eqs. (13) and (14) show that both PO and PC extrapolation errors vanish. When the ellipse transforms to a circle ( $\epsilon = 1$ ), the error for the PC method also vanishes. Thus, with reference to Fig. 1, if  $g(x) = f(x)$  and if the curve is a circle, the average of the begin-of-segment angle with the end-of-segment angle will always yield the chord angle  $\alpha_s$ .

The PO and PC methods approximated eight ellipses for which the minor/major axis ratios ranged from 1/1 (circle) to 1/20 (an ellipse with the major axis 20 times longer than the minor axis). The step length (SGU) was varied from 0.10–0.50 of the minor axis radius. Thus some ellipses were only 4 SGU wide when the maximum step length was used. Moreover, the analyses were rerun with the step increment positions shifted along the curves so as to avoid chance configurations that could give untypically small errors. It was found that the PC error

#### a. Error analysis for the ellipse

High and low pressure centers frequently perturb the troposphere at all levels. When the circulations associated with these pressure centers are nondivergent, the wind field streamlines should form closed curves. These curves are often nearly elliptical in shape. The individual and cumulative errors for a circuit around ellipses of varying eccentricity were calculated with (7) and (8). If we define the ellipse by

$$f(x) = -\epsilon^{-1}(a^2 - x^2)^{1/2}, \quad (10)$$

where  $\epsilon$  is the minor/major axis ratio and  $a$  is the minor axis radius, Eqs. (6) become

$$\left. \begin{aligned} f'(x_1) &= \frac{x_1}{\epsilon\beta_1} \\ f'(x_2) &= \frac{x_2}{\epsilon\beta_2} \\ \bar{f}'(x) &= -\frac{(\beta_2 - \beta_1)}{\epsilon(x_2 - x_1)} \end{aligned} \right\}, \quad (11)$$

where

$$\beta_1 = (a^2 - x_1^2)^{1/2}, \quad \beta_2 = (a^2 - x_2^2)^{1/2}. \quad (12)$$

The error for the predictor-only method is given by

$$R^+ = \frac{-\epsilon[\beta_1(\beta_2 - \beta_1) + x_1(x_2 - x_1)]}{\epsilon^2\beta_1(x_2 - x_1) - x_1(\beta_2 - \beta_1)} \quad (13)$$

After some manipulation, the predictor-corrector method error equation yields

was always smaller than the PO error and that the magnitudes of the analysis errors increased with curvature for both methods. The sign of the PO method analysis error was always positive, meaning that the curvature was always underestimated. Negative PC method errors gave curvature overestimates when the step increment was directed toward increasing curvature; curvature underestimates were found when the step increment was directed toward decreasing curvature.

The segment errors were summed to form the total analysis errors for one complete circuit around the ellipses. These cumulative errors were then normalized by dividing by the SGU. Table 1 expresses the maximum total error for the runs for each step length and minor/major axis ratio categories. The PO method curve gradually spiraled outward to a displacement of about 2 SGU at the completion of one

TABLE 1. Cumulative error for selected ellipses and step increment lengths. The errors have been normalized by dividing by the SGU.

Step increment*	Minor/major axis ratio							
	0.05	0.10	0.15	0.25	0.35	0.50	0.75	1.00
PO method								
0.10	2.10	2.00	2.00	2.00	2.00	2.00	2.00	2.00
0.25	2.52	2.12	2.08	2.08	2.04	2.04	2.04	2.12
0.50	2.78	2.94	2.36	2.34	2.28	2.28	2.34	2.14
PC method								
0.10	0.06	-0.01	-0.00	-0.00	-0.00	-0.00	-0.00	-0.00
0.25	0.54	0.11	-0.06	-0.00	-0.00	-0.00	-0.00	-0.00
0.50	0.74	0.64	0.12	0.06	0.09	0.02	0.01	-0.00

\* Step increment is given in fractions of minor axis radius.

circuit. Decreasing the SGU will decrease and make less objectionable the cumulative outward spiral.

Smaller PC method errors combine with a periodic overestimation and underestimation of curvature to almost totally compensate the error after one circuit. Total compensation did occur when the step increment positions on either side of an axis were made symmetrical.

As shown in Fig. 2, a SLX streamline initiated at  $S_{ij}$  must pass within 0.5 SGU of its initiation point (dashed box) for it to close upon itself and be terminated. Elliptical streamlines with error  $>0.5$  SGU will spiral outward unless some other method for termination is devised. According to Table 1, all PO and some PC streamlines will spiral outward. However, these PC curves will spiral outward to where the SGU is smaller relative to the minor axis radius, the cumulative error is less than 0.5 SGU, and the streamline is terminated.

PO and PC cumulative error behavior for three ellipses are shown in Fig. 3. The step increment was  $SGU = 0.5a$ . The cumulative errors for the respective minor/major axis ratios of 0.10, 0.25 and 0.50 for each method are shown on the last line in Table 1, respectively. The step sequence begins in

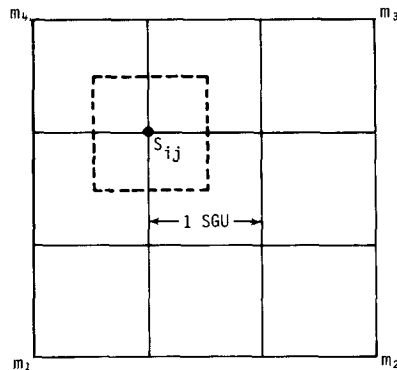


FIG. 2. Illustration of a nine-element subgrid within one element of a master grid.

the third quadrant and proceeds counterclockwise around the ellipses as is shown by the inset. PO and PC errors are largest at the curve apexes (at  $A = 0$ ) where the curvature maximizes. Compensation is seen for all PC error curves.

The proceeding analysis has shown that the PC method produces much smaller theoretical cumulative extrapolation errors for the ellipses than does the PO method. However, this analysis was based on the assumption that  $g(x) = f(x)$ , an assumption which is valid only for the straight line. For all other curves, the calculated end-of-segment angle  $\alpha_e$  in Fig. 1 will be equal to the true streamline exit angle  $\alpha_B$  for those few instances when the subgrid corner angles on the side of exit are equal. Otherwise some angular discrepancy exists and  $g(x) \neq f(x)$ .

The magnitude of the PC error that arises when this assumption is relaxed can be easily calculated for the circle which gave zero PC error for  $g(x) = f(x)$ . Streamlines for three circles of varying radii were constructed objectively by SLX. The coordi-

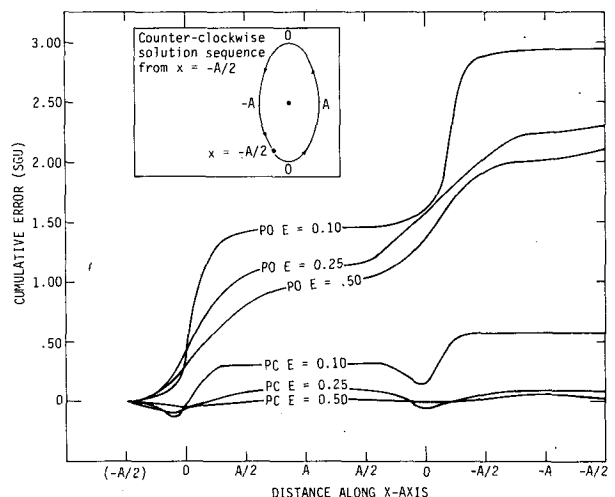


FIG. 3. PO and PC cumulative error curves for three ellipses.

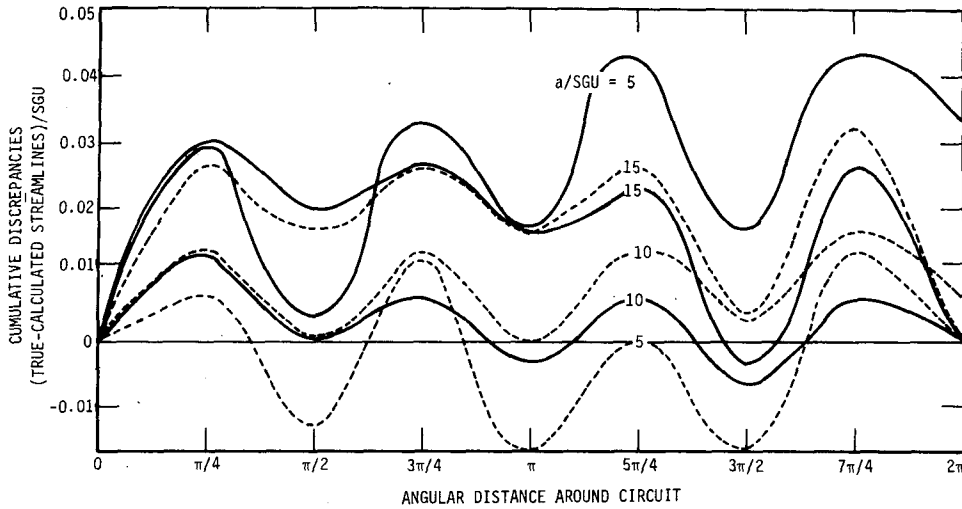


FIG. 4. Cumulative discrepancies between true and calculated streamlines for one circuit around circle of selected radii.

nates of the streamline at each step increment were compared with the corresponding coordinates on the analytical circle. The cumulative discrepancies are summarized in Fig. 4. The abscissa gives the angular distance in the mathematical framework for one complete circuit. The circles were constructed counterclockwise around the circuit (solid lines) after which the directions were reversed and the circles constructed clockwise around the circuit (dashed lines).

The cumulative error oscillates with a period of  $\pi/2$ . Streamlines spiral outward from  $0-\pi/4$  and spiral inward from  $\pi/4-\pi/2$  and so on. The total error for one circuit approaches zero for most of the streamlines. The variations in error amplitudes arise because the placement of the streamline segments within successive subgrid boxes varies between the curves. The maximum error is only a few

hundredths of a SGU and appears to be independent of the minor-axis-radius-to-step-increment ratio for the range of curves presented.

The reasoning of why the error oscillations occur is presented with the aid of Fig. 5 which shows in quadrant 4 a streamline that follows the circumference of a circle and passes through the two subgrid squares shown. When the center of the curve is located above and to the left of the subgrid square, the angle  $\gamma_3$  will always be the largest of the four corner angles. The streamline will more frequently exit through the side of the box in the interval from  $0-\pi/4$  and will more frequently exit through the top of the box in the interval from  $\pi/4$  to  $\pi/2$ . When the streamline exits through the side of the box, it will exit closer to the corner angle  $\gamma_3$  than will the PO segment ( $PO_1$ ). Thus the end-of-segment angle will be less than the actual streamline exit angle, the PC method will underestimate the curvature, and the objective streamline will spiral outward to a larger radius. When the streamline exits through the top of the box, the PO line will exit closer to  $\gamma_3$  than will the streamline. Here  $\alpha_e$  is greater than  $\alpha_B$ , the PC method overestimates the curvature, and the objective streamline spirals inward to a smaller radius. Under symmetric conditions, the cumulative error should vanish. Heuristically some compensation must occur for any closed curve regardless of the symmetry.

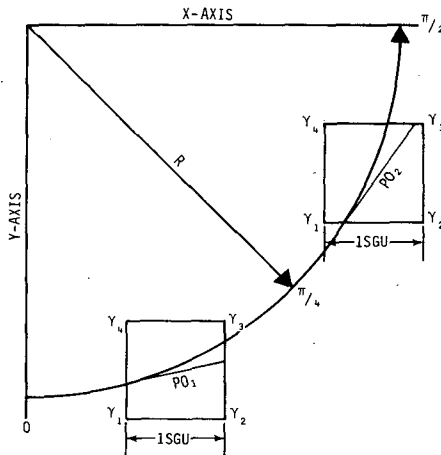


FIG. 5. Schematic diagram showing a streamline along the circumference of a circle passing through two subgrid squares.

*b. Error analysis for hyperbolic curves*

Hyperbolic curves are often found along trough lines, saddle points and other deformed flow fields. Fig. 6 shows five hyperbolas obtained from

$$f(x) = \delta^{-1} (r^2 + x^2)^{1/2}. \tag{15}$$

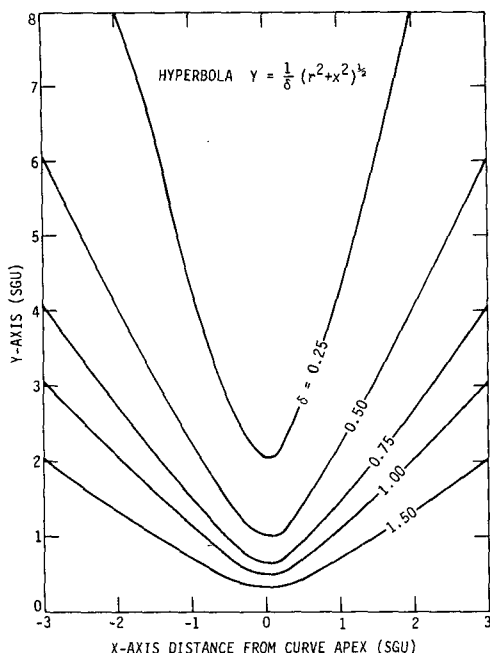


FIG. 6. Hyperbolas used for the PO and PC method error analysis.

These curves are but a small sample of the infinite number of possible hyperbolic curves, yet they contain the range of apex curvature variations necessary to demonstrate the accuracies of the PO and PC methods. Following the theoretical developments outlined in the previous section, the PO and PC hyperbola error equations were developed. Both methods gave zero error for  $\delta = 0$  and  $\delta = \infty$ , i.e., the straight line solutions.

The cumulative error curves for a step increment sequence that proceeds from the left to the right through the curve apexes are shown in Fig. 7. Maximum theoretical error was found in the region of maximum curvature. Elsewhere, the error was negligibly small. The smaller PC method errors compensated and were about an order of magnitude less than the PO method error; however, the latter still produced errors less than a subgrid unit. The PO method underestimated curvature at all points along the curves. The PC method overestimated curvature as the solution sequence proceeded toward the apex and afterward overestimated the curvature. As shown in Fig. 7, the PC cumulative error for most of the hyperbolas tested was nearly zero.

*c. Error analysis for sine waves*

Theoretical streamline errors were obtained for a matrix of sine waves that were varied in amplitude and wavenumber. Amplitudes ranged from 1–10 SGU and the wavelengths were varied from 15 SGU (wavenumber 1) to 3.75 SGU (wavenumber 4). Thus, the shortest wavelength was less than four

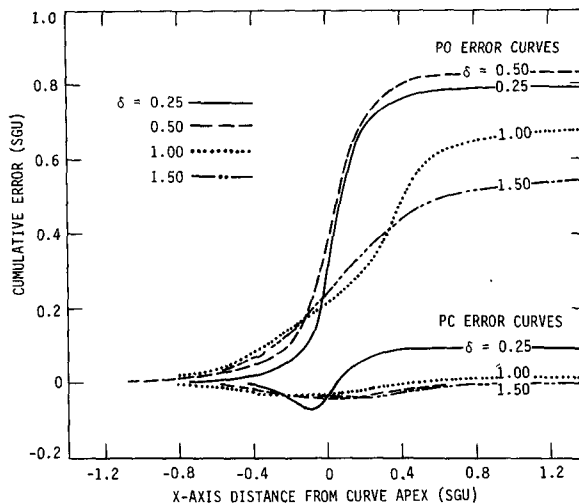


FIG. 7. PO and PC method cumulative errors for selected hyperbolas. See text for explanation.

subgrid spaces long. This would be the smallest resolvable wave if the master grid mesh length were twice the subgrid mesh length.

The theoretical error for the zero-amplitude wave (straight line) was zero. For all nonzero amplitudes, some error was found, although for some curves, it was negligibly small. Table 2 summarizes the PO and PC cumulative error for 16 sine waves. The step increment was 1 SGU. The errors are small for both methods; errors ranged from near zero to a few tenths of a subgrid unit. There was no discernable trend for errors to increase either with amplitude or with wavenumber. The nearly random distribution of error magnitudes and signs arose because of the placement of the step increment end points along the curves.

The cumulative error distributions along the wavenumber 2, amplitude 4 sine wave are shown in Fig. 8. The PO method consistently underestimated the curvature but the curvature changed sign and the total error compensated to leave only a slight phase shift. Maximum individual increment errors reached 1.5 SGU in some instances. The PC method consistently compensated its errors according to the

TABLE 2. PO and PC method cumulative errors for sine waves of selected amplitude and wavelength. Error is in fractions of a SGU.

Wave-number	Amplitude (SGU)							
	PO method				PC method			
	1	4	7	10	1	4	7	10
1	-0.00	-0.00	0.01	0.03	0.00	0.00	-0.02	-0.02
2	-0.00	-0.02	0.11	0.12	0.00	0.10	-0.28	-0.01
3	-0.06	0.14	-0.10	0.12	-0.01	-0.03	0.15	-0.13
4	-0.22	-0.11	-0.06	0.09	-0.12	0.15	0.12	-0.08

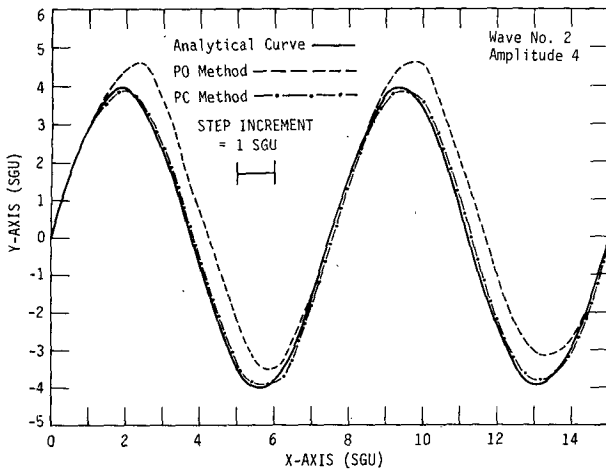


FIG. 8. PO and PC method cumulative errors for the wavenumber 2, amplitude 4 sine wave. See text for explanation.

trend in curvature. This led to small error at all points along the curve.

#### 4. Concluding remarks

This theoretical study was limited by the small number of possible curves that were theoretically formulated for the error analysis. Hence, no absolute proof that no curve will produce unacceptably large analysis error is given. However, inasmuch as each curve segment can be represented by a segment or a linear combination of segments from the curve families presented in this study, the segment error should not greatly exceed the errors shown.

The ellipse, hyperbola and sine wave curves were selected to be representative of meteorological flow patterns and to show large curvatures near the minimum resolvable scale limitations of the master grid so to give an estimate of the largest errors to be expected. PC errors were always smaller than PO errors. The PO method consistently underestimated the actual streamline curvature. For closed curves such as the ellipse, this will develop an outward spiral that could be objectionable unless the step increment is made small. The PC method overestimated curvature where the step increment was directed toward increasing curvature and underestimated curvature where the step increment was directed toward decreasing curvature. This led to error compensation for all curves studied. Heuristically, compensation should occur for all curves except the spiral for which the curvature always increases or decreases depending on the direction of the streamline.

Now, how do these results translate into accuracy and economics for operations? It has been shown that, with regard to the method of line segment extrapolation, the PC method is clearly superior to the PO method. Perhaps, with some minor modifications,

many techniques based on PO can be easily converted to PC. The conversion will be accompanied by a modest increase in CPU time because more computations are required to develop the PC line segments. PO and PC test runs with the SLX with equivalent step increments reveal that increases of ~11% in CPU time should be expected.

Perhaps, however, the accuracy of the PO method can be increased by decreasing the step increment locally in areas of large curvature. With regard to the ellipse, the reduction in the PO step increment necessary to achieve an equivalent accuracy with the PC method can be easily found. From Table 1, the PO error ( $E_{PO}$ ) is approximately 2.00 SGU for most step increments and minor-to-major-axis ratios. Therefore, the PO step increment required to duplicate the accuracy of the PC method at a specified step increment can be determined from  $S_{new} = S_{old}(E_{PO}/E_{PC})$ . The PO step increment in the areas of sharp curvature would have to be 20 times shorter than the PC step increment for the step increment = 0.25, minor-to-major axis ratio = 0.10, ellipse-step increment combination. Further, as the minor-to-major-axis ratio increases, the PC error vanishes (to within truncation) and infinitesimally small PO step increments would be required along the entire length of the curve to achieve comparable accuracy.

The increase in the number of PO line segments to achieve equivalent accuracy would at least partially and, for some curves, more than offset the complexity of the PC method in CPU time consumed. On the other hand, if satisfactory accuracy is being obtained from a currently operational PO method, conversion to PC and lengthening the step increment could realize a substantial savings.

*Acknowledgments.* Stimulating conversations with Dr. S. L. Barnes during the early phases of this research while the author was a National Research Council Post Doctoral Research Associate at the National Severe Storms Laboratory are greatly appreciated. The later phases of the research were done under the general supervision of S. A. Changnon, Jr., Head, Atmospheric Sciences Section, Illinois State Water Survey, and supported by the Atmospheric Water Resources Management Division of the Bureau of Reclamation under Contract 14-06-D-7197 (High Plains Experiment Design Project).

#### APPENDIX

##### An Operational Objective Streamline Analysis

The objective streamline analysis (SLX) was developed at the National Severe Storms Laboratory<sup>2</sup>

<sup>2</sup> This phase of the work was completed while the author was a National Research Council Post-Doctoral Research Associate at the National Severe Storms Laboratory.

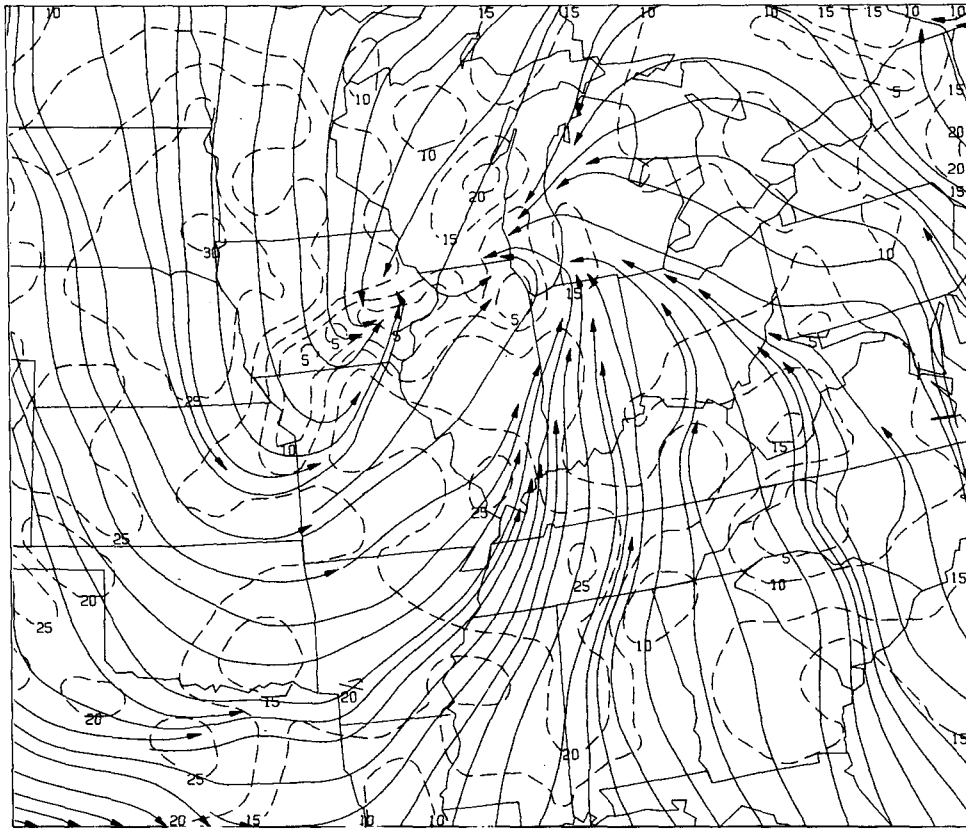


FIG. 9. SLX streamlines of the surface wind field for 1500 CST 3 April 1974. Dashed lines are isotachs (kt). ( $1 \text{ m s}^{-1} = 1.98 \text{ kt}$ .)

and placed into operation there in the spring of 1973. In 1976, the SLX was reprogrammed at the Illinois State Water Survey (Achtemeier *et al.*, 1978) and adapted for use on the Bureau of Reclamation Environmental Data Network (Politte *et al.*, 1977). Some examples of the SLX may be found in Achtemeier (1975), Heymsfield (1976), Ray (1976), Goff (1976), Brown (1976), Barnes (1974) and Merritt *et al.* (1974).

The SLX method uses two master arrays that contain  $u$  and  $v$  wind components at mesh points of a regular grid. The wind components are bilinearly interpolated to the points of a subgrid mesh and there converted to directions. The number of subgrid intervals per master grid interval is an integer which is chosen with regard to curve smoothness, computer memory limitations and cost per analysis. An additional subgrid that contains the streamline identifier symbols is also required for the analysis.

Fig. 2 illustrates a nine-element subgrid within one element of the master grid. If a streamline passes through the dashed line square centered about the subgrid point  $s_{ij}$ , its unique identifier is recorded at that point in the identifier array. If that point already contains the identifier for another streamline, the streamline is terminated.

A streamline can be started at any subgrid point provided it is not within some specified distance from another streamline. The density of the streamlines is determined by the analyst. Once a starting point for a new streamline is established, the streamline is drawn in two directions: first forward and then backward by reversing the unit direction vector  $180^\circ$ . The streamline is a succession of straight line segments; the segment lengths are determined by the entry and exit points through the subgrid squares.

The streamline is terminated when 1) it intersects the boundary of the master grid; 2) it comes within half of the subgrid interval of a grid point containing the identifier of another streamline; 3) it comes within half of the subgrid interval of a grid point containing its identifier (the streamline intersects itself); and 4) the angle between two successive line segments exceeds  $90^\circ$ . Here streamlines are terminated to prevent "sawtooth" curves from being constructed at the interface between air masses with opposing flow.

The streamlines can be displayed by some automated line drawing device or by listing the array of unique identifier symbols on a line printer. Fig. 9 shows an example of the SLX streamline analysis.



## REFERENCES

- Achtemeier, G. L., 1975: On the initialization problem—A variational adjustment method. *Mon. Wea. Rev.*, **103**, 1089–1103.
- Achtemeier, G. L., P. H. Hildebrand, P. T. Schickedanz, B. Ackerman, S. A. Changnon, Jr., and R. G. Semonin, 1978: Illinois precipitation enhancement program (Phase 1) and design and evaluation techniques for High Plains Cooperative Program. Atmos. Sci. Sec., Illinois State Water Survey, Final Rep., Contract 14-06-D-7197, 313 pp.
- Barnes, S. L., 1974: Papers on Oklahoma thunderstorms, April 29–30, 1970. NOAA Tech. Memo. ERL NSSL-69, Norman, National Severe Storms Laboratory, 233 pp. [NTIS COM-74-11474].
- Brown, R. A., Ed., 1976: The Union City, Oklahoma tornado of 24 May 1973. NOAA Tech. Memo. ERL NSSL-80, Norman, National Severe Storms Laboratory, 234 pp. [NTIS PB-269-443].
- Daart, D. G., 1972: Automated streamline analysis utilizing "optimum interpolation." *J. Appl. Meteor.*, **11**, 901–908.
- Davis, R. A., 1969: A computer method to generate and plot streamlines. USWB Pacific Region, ESSA, Tech. Memo. WBTM PR-5, 12 pp. [NTIS PB-183-162].
- Goff, R. C., 1976: Vertical structure of thunderstorm outflows. *Mon. Wea. Rev.*, **104**, 1429–1440.
- Heymsfield, G. M., 1976: Statistical objective analysis of dual-Doppler radar data from a tornadic storm. *J. Appl. Meteor.*, **15**, 59–68.
- Merritt, L. P., K. E. Wilk and M. L. Weible, 1974: Severe rainstorm at Enid, Oklahoma—October 10, 1973. NOAA Tech. Memo. ERL NSSL-73, 50 pp. [NTIS COM-75-10583].
- Politte, F. E., M. D. Hale and D. A. Matthews, 1977: The Bureau of Reclamation's Environmental Data Network. *Preprints, 6th Conf. Planned and Inadvertent Weather Modification, Champaign-Urbana*, Amer. Meteor. Soc., 362–363.
- Ray, P. S., 1976: Vorticity and divergence fields within tornadic storms from dual-Doppler observations. *J. Appl. Meteor.*, **15**, 879–890.
- Saucier, W. J., 1955: *Principles of Meteorological Analysis*. The University of Chicago Press, 438 pp.
- Whittaker, T. M., 1977: Automated streamline analysis. *Mon. Wea. Rev.*, **105**, 786–788.